

Piezo-phototronic effect on intersubband optical absorption in ZnO/MgZnO quantum wells

Yuchang Liu(刘羽畅), Jiuzhou Chen(陈九州), Yonglong Yang(杨永龙), Xiaolong Pan(潘小龙), Xin Xue(薛鑫), Minjiang Dan(但敏江), Zhengwei Xiong(熊政伟), and Zhipeng Gao(高志鹏)

Citation: Chin. Phys. B, 2025, 34 (**8**): 087802. DOI: 10.1088/1674-1056/adce93
http://cpb.iphy.ac.cn; http://iopscience.iop.org/cpb

What follows is a list of articles you may be interested in

Enhanced absorption process in the thin active region of GaAs based p-i-n structure

Chen Yue(岳琛), Xian-Sheng Tang(唐先胜), Yang-Feng Li(李阳锋), Wen-Qi Wang(王文奇), Xin-Xin Li(李欣欣), Jun-Yang Zhang(张珺玚), Zhen Deng(邓震), Chun-Hua Du(杜春花), Hai-Qiang Jia(贾海强), Wen-Xin Wang(王文新), Wei Lu(陆卫), Yang Jiang(江洋), and Hong Chen(陈弘)

Chin. Phys. B, 2021, 30 (**9**): 097803. DOI: 10.1088/1674-1056/abf10c

Effects of substitution of group-V atoms for carbon or silicon atoms on optical properties of silicon carbide nanotubes

Ying-Ying Yang(杨莹莹), Pei Gong(龚裴), Wan-Duo Ma(马婉铎), Rui Hao(郝锐), and Xiao-Yong Fang(房晓勇)

Chin. Phys. B, 2021, 30 (**6**): 067803. DOI: 10.1088/1674-1056/abdb1e

Optical properties of core/shell spherical quantum dots

Shuo Li(李硕), Lei Shi(石磊), Zu-Wei Yan(闫祖威)

Chin. Phys. B, 2020, 29 (**9**): 097802. DOI: 10.1088/1674-1056/ab961a

Effects of built-in electric field and donor impurity on linear and nonlinear optical properties of wurtzite $In_xGa_{1-x}N$/GaN nanostructures

Xiao-Chen Yang(杨晓晨), Yan Xing(邢雁)

Chin. Phys. B, 2020, 29 (**8**): 087802. DOI: 10.1088/1674-1056/ab9291

SnS_2 quantum dots: Facile synthesis, properties, and applications in ultraviolet photodetector

Yao Li(李尧), Libin Tang(唐利斌), Rujie Li(李汝劼), Jinzhong Xiang(项金钟), Kar Seng Teng, Shu Ping Lau(刘树平)

Chin. Phys. B, 2019, 28 (**3**): 037801. DOI: 10.1088/1674-1056/28/3/037801

Piezo-phototronic effect on intersubband optical absorption in ZnO/MgZnO quantum wells

Yuchang Liu(刘羽畅)[1,†], Jiuzhou Chen(陈九州)[2,†], Yonglong Yang(杨永龙)[2,†], Xiaolong Pan(潘小龙)[2], Xin Xue(薛鑫)[3], Minjiang Dan(但敏江)[2,‡], Zhengwei Xiong(熊政伟)[2,§], and Zhipeng Gao(高志鹏)[2,4,¶]

[1] *School of Physics, Nanjing University of Science and Technology, Nanjing* 210094, *China*
[2] *Joint Laboratory for Extreme Conditions Matter Properties, School of Mathematics and Physics, Southwest University of Science and Technology, Mianyang* 621010, *China*
[3] *Department of Physics, Lvliang University, Lvliang* 033000, *China*
[4] *Institute of Fluid Physics, China Academy of Engineering Physics, Mianyang* 621900, *China*

(Received 9 January 2025; revised manuscript received 13 April 2025; accepted manuscript online 21 April 2025)

Intersubband transition in ZnO/MgZnO quantum well has been exploited for infrared and terahertz optoelectronic applications due to its large band offset and fascinating material properties. Here, we theoretically demonstrate piezo-phototronic effect as another way to control the intersubband absorption wavelength through quantum-confined Stark effect. The intersubband optical absorption properties under different stresses are obtained by solving the eight-band $k \cdot p$ Hamiltonian and coupled Schrödinger–Poisson equations self-consistently. By combining stress control and quantum well structure, the absorption wavelength can show infrared blueshift or redshift phenomena in a wide range. This work can provide an effective avenue to control and utilize quantum-confined Stark effect in intersubband infrared absorption and promote the relative potential optoelectronic devices.

Keywords: ZnO/MgZnO quantum well, intersubband transition, piezo-phototronic effect, optical absorption

PACS: 78.67.De, 78.20.hb, 71.35.Cc

DOI: 10.1088/1674-1056/adce93 **CSTR:** 32038.14.CPB.adce93

1. Introduction

ZnO is a typical wide-band-gap semiconductor with large exciton binding energy (∼ 60 meV) which plays an essential role in optoelectronic devices such as ultraviolet lasers and light-emission diodes.[1–5] Ternary alloy MgZnO shows a band gap varying from 3.3 eV to 7.8 eV controlled by doping and temperature.[6,7] Besides, ZnO and MgZnO semiconductors can form quantum well structure with good lattice mismatch, which has potential for quantum well laser applications.[8] Large conduction band offset (∼ 1.0 eV) between MgZnO and ZnO allows for intersubband optical transitions in ZnO-based quantum wells operating over a wide spectrum range.[6,9] ZnO/MgZnO quantum well was firstly achieved intersubband transition in experiment by Ohtani in 2009.[10] The infrared absorption wavelength ranges from 3.3 μm to 4.3 μm for ZnO/MgZnO quantum well with 40% Mg composition by varying the quantum well width.[11] The intersubband absorption wavelength is tunable depending on the doping, temperature and quantum well structure.[10,12] Besides, decreasing barrier thickness leads to weakened built-in electric field in the well layer, resulting in shorter interband emission wavelength.[12] As a result, changing the internal electric field provides an effective method to control the optical absorption properties through the quantum-confined Stark effect.

Both ZnO and MgZnO are wurtzite materials with piezoelectric property. The influence of spontaneous polarization and strain-induced piezoelectric polarization can introduce a strong electric field (∼ MV/cm) across the quantum well layer.[13–15] Then, the density of two-dimensional electron gas (2DEG) localized at the interface can reach up to 10^{13} cm^{-2}.[16,17] By increasing the well thickness, the excitonic transition energy decreases and shows a redshift in ZnO quantum wells due to the quantum-confined Stark effect caused by the weakened internal electric field.[18–21] Benefiting from the piezotronic and piezo-phototronic effects widely applied in piezoelectric semiconductors, one can utilize the stress-induced polarized electric field to control the electric and optical properties through the coupling of piezoelectricity, photoexcitation and semiconductor.[22,23] For example, the externally applied pressure can cause the redshift of intersubband absorption wavelength from 1.6 μm to 2.2 μm in GaN/AlN wurtzite quantum wells.[24] The maximum of normalized photoluminescence intensity decreases

[†]These authors contributed equally to this work.
[‡]Corresponding author. E-mail: minjiang.dan@swust.edu.cn
[§]Corresponding author. E-mail: zw-xiong@swust.edu.cn
[¶]Corresponding author. E-mail: z.p.gao@foxmail.com

© 2025 Chinese Physical Society and IOP Publishing Ltd. All rights, including for text and data mining, AI training, and similar technologies, are reserved.

from 1 to 0.5 when applying −0.4% strain along c axis in InGaN/GaN quantum wells.[25] Compared with GaN quantum well, ZnO/MgZnO quantum well has larger exciton binding energy which is beneficial for the realization of room temperature exciton effect and optoelectronic applications.[26] However, externally stress-induced piezo-phototronic effect is less studied in ZnO/MgZnO quantum well although it is a suitable platform for intersubband transition with strong piezoelectric property.

In this work, we conduct theoretical study towards intersubband optical absorption in ZnO/MgZnO quantum wells under stress-induced piezoelectric polarization field. Through self-consistently solving the coupled Schrödinger–Poisson equations from eight-band $k \cdot p$ Hamiltonian, the conduction band potential profile and intersubband optical absorption properties are obtained under various stresses. Stress can increase the internal built-in electric field in the quantum well structure and cause a blueshift or redshift of absorption wavelength depending on the well structure. We also explicitly study the influence of stress and quantum well structure (well and barrier thickness) on the intersubband optical absorption. This work not only discusses the piezo-phototronic effect on intersubband optical absorption in ZnO/MgZnO quantum wells, but also provides another guidance to design optoelectronic devices based on quantum well structure.

2. Wurtzite ZnO/MgZnO quantum well structure

ZnO/MgZnO quantum well can be grown by plasma-assisted molecular beam epitaxy (PAMBE) or pulsed laser deposition (PLD) technique.[27,28] A single quantum well consists of one ZnO well layer and two MgZnO barrier layers and ZnO layer is sandwiched between two MgZnO layers to drive intersubband transition, as shown in Fig. 1(a). For the natural case, spontaneous polarization and piezoelectric polarization can produce a strong built-in electric field across the well layer (see the left of Fig. 1(a)). This phenomenon has been widely revealed in ZnO/MgZnO and other quantum well structures.[21,29,30] As a consequence of built-in electric field, the conduction band potential profile shows an incline and free electrons are trapped as shown in the right of Fig. 1(a). The arrow indicates a typical intersubband optical transition from ground state e_1 to first excited state e_2 when a suitable light with specific wavelength is incident. Here, we only focus on the transition from e_1 to e_2 due to their high oscillator strength under selection rules. Hydrostatic pressure is a commonly used way in experiment to supply pressure and further induce strain in ZnO/MgZnO quantum well structure.[31,32] When an external stress is applied on the quantum well along c axis, stress-induced piezoelectric polarization charges are localized at the interface as shown in the left of Fig. 1(b). As a result, the built-in electric field will be further enhanced by piezoelectric field as shown in the right of Fig. 1(b), leading to the increased intersubband transition energy between two confined states, e_1 and e_2.

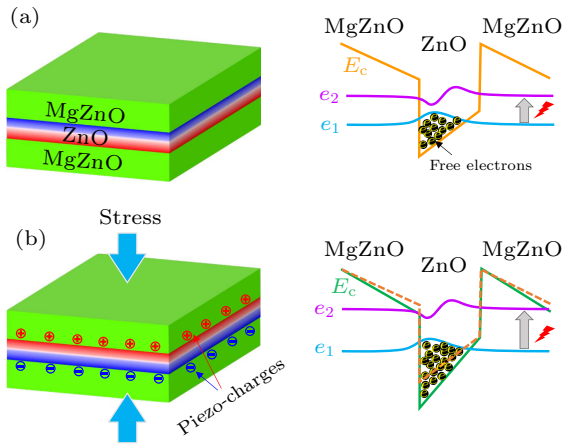


Fig. 1. Schematic diagram of ZnO/MgZnO quantum well and conduction band potential profile (a) without stress, and (b) with stress. e_1 and e_2 are ground state and first excited state, respectively. Intersubband transition occurs between e_1 and e_2 states under specific incident light. Green line shows the case after stress is applied.

In the following, we will first introduce the basic theory used in this study and then discuss the relevant results.

3. Basic theory and model

In polar quantum wells, polarized electric field exists in the well and barrier layers due to spontaneous polarization P^{sp} and piezoelectric polarization P^{pz}. Piezoelectric polarization depends on the endured strain $P^{\mathrm{pz}} = \boldsymbol{e} \cdot \boldsymbol{s}$, where $\boldsymbol{e}$ is the tensor of piezoelectric constant and $\boldsymbol{s}$ is the vector of strain. And strain comes from lattice mismatch as well as externally applied stress in heterostructure system. For wurtzite quantum well grown along c-axis direction, the lattice-mismatched strain is obtained from $s_{xx} = s_{yy} = (a - a_{\mathrm{sub}})/a_{\mathrm{sub}}$, $s_{zz} = -2s_{xx}C_{13}/C_{33}$, where a and a_{sub} are lattice constants of quantum well material and substrate, C_{13} and C_{33} are elastic coefficients.[33,34] Additionally, strain introduced by externally applied stress can be deduced according to the strain–stress relationship $\boldsymbol{\sigma} = \boldsymbol{C} \cdot \boldsymbol{s}$, where $\boldsymbol{\sigma}$ is the stress vector and $\boldsymbol{C}$ is the tensor of elastic coefficient. Once obtaining the total polarization in quantum well, we can get the built-in electric field in well and barrier following the condition $d_{\mathrm{b}}E_{\mathrm{b}} + d_{\mathrm{w}}E_{\mathrm{w}} = 0$, with thickness d_{b} and electric field E_{b} for barrier layer, d_{w} and E_{w} for well layer.[35,36]

To get subband levels and wavefunctions for the quantum well system, we need to start from one-dimensional (1D) Schrödinger equation which is given as

$$[H(z) + V(z)]\,\psi_n(z) = E_n\psi_n(z), \tag{1}$$

where $V(z) = -q\varphi(z) + V_{\mathrm{ex}}$ is the total potential energy, $\varphi(z)$ is the built-in electric potential, and V_{ex} is the exchange–correlation potential[37] and $H(z)$ is the Hamiltonian of ZnO

and MgZnO. For obtaining higher accurate solutions, eight-band $k\cdot p$ Hamiltonian accounting for band nonparabolicity is adopted here.[38–40]

The 1D Poisson equation for the quantum well to get potential distribution can be denoted as[41]

$$\frac{\mathrm{d}D(z)}{\mathrm{d}z} = q\left[N_{\mathrm{D}}(z) - n(z)\right], \tag{2}$$

where the displacement field $D(z) = P_{\mathrm{total}} - \varepsilon_{\mathrm{r}}\varepsilon_0 \mathrm{d}\varphi/\mathrm{d}z$, P_{total} is the total polarization including piezoelectric polarization and spontaneous polarization, ε_{r} and ε_0 are relative and vacuum permittivity, φ is the built-in electrostatic potential, q is electron charge, N_{D} is the ionized donor density and n is free electron density. The free electron density n is associated with energy level and wavefunction of quantized subbands from the relationship[36]

$$n(\mathrm{z}) = \sum_{m=1}^{\infty} n_m \left|\psi_m(z)\right|^2, \tag{3}$$

where ψ_m is the wave function of the m-th subband, n_m is two-dimensional (2D) density of state which is given by $n_m = \iint f_m(k_x, k_y)\,\mathrm{d}k_x\mathrm{d}k_y$, where k_x and k_y are 2D wave vector. $f_m = [1+\exp((E_m - E_{\mathrm{F}})/kT)]^{-1}$ is Fermi–Dirac function, where E_m is the energy level of the m-th subband, E_{F} is the Fermi energy, k is the Boltzmann constant, and T is temperature. The Fermi energy is obtained from charge neutrality condition $\int [N_{\mathrm{D}}(z) - n(z)]\,\mathrm{d}z{=}0$, which is integrated over single quantum well.

After the needed initial parameters are prepared, the Schrödinger equation is solved under periodic boundary conditions with a trial potential to obtain the subband energies and wavefunctions. Fermi energy is calculated with charge neutrality condition over one period of the quantum well. Then, subband populations and exchange–correlation potential are obtained based on subband energies, wavefunctions and Fermi energy. The Poisson equation is solved under proper boundary conditions to get the potential energy caused by polarization field and doping. Finally, exchange–correlation potential and potential energy are used to update the initial trial potential. The above procedure is repeated until the convergence is achieved and the detailed self-consistent process can be found in Ref. [36].

After a self-consistent iteration process of the coupled Schrödinger equation and Poisson equation, the absorption coefficient of intersubband optical transition is given as[34,36,42]

$$\alpha = \frac{A}{\omega}\sum_{m=1}^{M}\sum_{n=1}^{N}\int \left|M_{mn}(k=0)\right|^2 \times \left[f_m(k) - f_n(k)\right] g\left(\Delta E_{mn}, \hbar\omega\right)\frac{k\mathrm{d}k}{2\pi}, \tag{4}$$

where ω is the incident radiation angular frequency, M and N are the numbers of initial and final subbands during intersubband transition, A is a frequency-independent constant $A = q^2\pi/(n_{\mathrm{r}}c\varepsilon_0 m_0^2 d_{\mathrm{w}})$ where n_{r} is the refractive index, c is the velocity of light and m_0 is the rest mass of an electron, g is the Lorentzian function, $\hbar$ is the reduced Planck constant, $\Delta E_{mn} = E_m - E_n$ is the transition energy between the n-th state (E_n) and the m-th state (E_m), $M_{mn} = \frac{m_z(E_m - E_n)}{\mathrm{i}\hbar}\langle\psi_m|z|\psi_n\rangle$ is the momentum matrix element, m_z is electron effective mass along c-axis direction.

4. Results and discussion

For demonstrating piezo-phototronic effect on intersubband optical absorption in ZnO/ MgZnO quantum well, we take an experimentally commonly-used ZnO/$Mg_{0.23}Zn_{0.77}O$ quantum well structure consisting of ZnO layer $d_{\mathrm{w}} = 2.0$ nm and $Mg_{0.23}Zn_{0.77}O$ layer $d_{\mathrm{b}} = 3.3$ nm.[27,43] For simplicity, $Mg_{0.23}Zn_{0.77}O$ is simplified to MgZnO without explicit mention. ZnO is n-doped with the concentration $N_{\mathrm{D}} = 10^{19}$ cm^{-3} and $Mg_{0.23}Zn_{0.77}O$ is unintentionally doped. The temperature is fixed at $T = 18$ K in order to compare with experiments.[27] Previous studies have revealed that temperature fluctuations have less impact on piezotronic effect and intersubband absorption wavelength is relatively stable under temperature fluctuations.[44–47]

Figure 2(a) illustrates conduction band potential profiles of single ZnO/MgZnO quantum well under externally applied stress varying from 0 to 20 GPa. The potential at right interface is set as reference point to compare the potential change for clarity. As it can be seen, the built-in electric field is enhanced with increasing stress and the band offset is also influenced by stress. The potential profile is heavily inclined in the whole quantum well due to the spontaneous polarization and lattice-misfit-induced piezoelectric polarization without external stress. The initial built-in electric fields are around 2.7 MV/cm and 1.6 MV/cm in the well and barrier layer, respectively (see Fig. 2(b)). The electric field increases linearly in the opposite direction as a function of increasing stress.

Such enhanced electric field can bring in quantum-confined Stark effect for intersubband optical absorption as shown in Fig. 2(c).[48,49] The absorption spectrum is located in infrared region close to 3.0 μm without stress, which is in good agreement with experimental measurements.[10,27] As it can be seen, the absorption spectra exhibit a blueshift with increasing stress. The absorption wavelength is shifted to around 2.9 μm under 20-GPa stress. This phenomenon can be well understood because the increasing built-in electric field enhances quantum confinement of quantum well which is similar to the reduction of ZnO well thickness.[11,27,50] Figure 2(d) plots the absorption wavelength decreased from 3.02 μm to 2.91 μm with increasing stress. Compared with intersubband absorption modulation methods, such as electric field modulation and structural parameter modulation, pressure-induced piezo-phototronic effect can precisely and continuously control the absorption wavelength.[24,31,32,51]

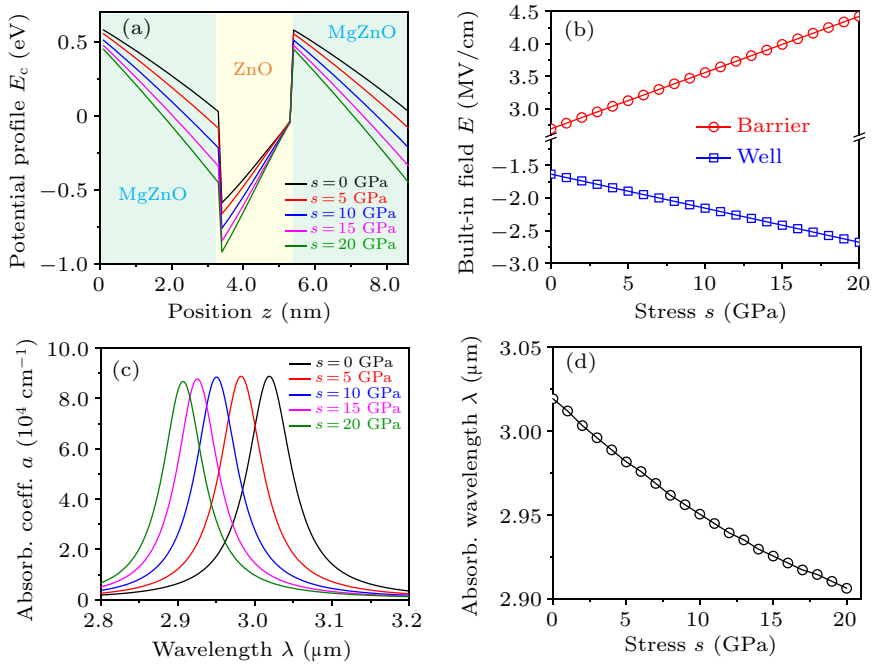


Fig. 2. (a) Stress-dependent potential profiles in single ZnO/MgZnO quantum well. (b) Stress-dependent polarization field in well and barrier layer. (c) Absorption spectrum under different stresses, and (d) absorption wavelength *versus* stress. The quantum well consists of 2.0-nm ZnO and 3.3-nm MgZnO, n-doping 1×10^{19} cm^3 in ZnO layer. Temperature is fixed at $T = 18$ K.

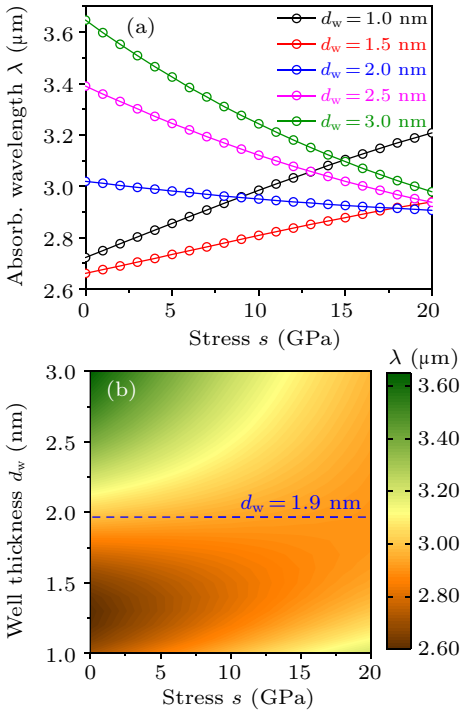


Fig. 3. (a) Absorption wavelength *versus* stress under different well thicknesses d_w and barrier thickness is fixed at $d_b = 3.3$ nm. (b) Contour plot of absorption wavelength as a function of stress and well thickness ($d_b = 3.3$ nm).

Since the built-in electric field in polar quantum wells is also dependent on the thickness of well layer,[10,21,52] here we also conduct systematic study about the influence of quantum well structure on intersubband optical absorption (well and barrier thickness). Figure 3(a) displays the absorption wavelength as a function of stress at different well thicknesses (1.0 nm, 1.5 nm, 2.0 nm, 2.5 nm and 3.0 nm) with a fixed barrier thickness $d_b = 3.3$ nm. When the well thickness is small, such as 1.0 nm and 1.5 nm, the absorption wavelength shows redshift with increasing stress instead of blueshift as discussed before. This is because the well thickness is too small to confine the first excited energy level and applied stress have more impact on ground state rather than first excited state, leading to redshift.[51] Otherwise, the first excited state is confined into the quantum well when the quantum confinement effect is weakened by large well thickness, stress-induced piezo-phototronic effect can enhance the built-in electric field and lead to the blueshift of absorption wavelength. If we continually change the well thickness in a small step, we can find out the critical well thickness to confine the first excited state as shown in Fig. 3(b). This critical well thickness is around 1.9 nm as indicated by the dotted line. When the well thickness is larger than 1.9 nm, the intersubband absorption wavelength shows a blueshift with increasing stress.

Figure 4(a) plots the intersubband absorption wavelength as a function of applied stress for different barrier thicknesses (3.0 nm, 3.5 nm, 4.0 nm, 4.5 nm, and 5.0 nm) at a fixed well thickness $d_w = 2.0$ nm. As we can see, barrier thickness can also affect the dependence of absorption wavelength on stress. The absorption wavelength slightly increases with increasing barrier thickness because the adopted well thickness is small, as observed in GaN/AlN multiple quantum wells.[53] Applied stress can lead to the blueshift for absorption wavelength when the barrier thickness is small. While for large barrier thickness (like 5.0 nm), the absorption wavelength slightly decreases and then increases *versus* stress. This may be caused by the large quantum confinement effect and only ground state is trapped into the quantum well under large stress. Figure 4(b) shows the impact of both barrier thickness and external stress on the absorption wavelength. The influence of barrier thickness on absorption wavelength is less than that of well thickness. And

stress can control the absorption wavelength in a wide range at small barrier thickness.

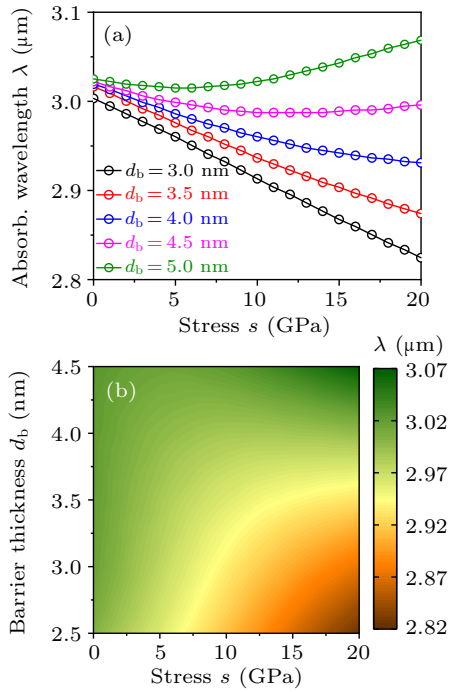


Fig. 4. (a) Absorption wavelength *versus* stress under different barrier thicknesses d_b and well thickness is fixed at $d_w = 2.0$ nm. (b) Contour plot of absorption wavelength as a function of stress and barrier thickness ($d_w = 2.0$ nm).

5. Conclusion

We theoretically studied the impact of piezo-phototronic effect on intersubband optical absorption in ZnO/MgZnO quantum well structure. Using eight-band $k \cdot p$ method and self-consistent solution of coupled Schrödinger–Poisson equations, the band profile and intersubband transition spectra are obtained under various external stresses. The results show that external stress has significant impact on intersubband optical absorption wavelength. Furthermore, we simultaneously change quantum well structure and external stress to investigate their effects on intersubband optical absorption wavelength in quantum well. This work not only vividly illustrates the piezo-phototronic effect on intersubband optical absorption in ZnO/MgZnO quantum well, but also sheds a new light on ways to continuously regulate the optical absorption wavelength in quantum well devices.

Acknowledgements

Project supported by the National Natural Science Foundation of China (Grant Nos. U2430204, U23A20567, and U2230119) and the Outstanding Youth Science and Technology Talents Program of Sichuan Province, China (Grant No. 22JCQN0005).

References

[1] Sun H D, Makino T, Segawa Y, *et al*. 2002 *J. Appl. Phys.* **91** 1993
[2] Ryu Y, Lee T S, Lubguban J A, *et al*. 2006 *Appl. Phys. Lett.* **88** 241108
[3] Willander M, Nur O, Zhao Q X, *et al*. 2009 *Nanotechnology* **20** 332001
[4] Van Vugt L K, Ruhle S, Ravindran P, *et al*. 2006 *Phys. Rev. Lett.* **97** 147401
[5] Teisseyre H, Jarosz D, Marona L, *et al*. 2020 *Phys. Status Solidi (a)* **218** 202000344
[6] Ohtomo A, Kawasaki M, Koida T, *et al* 1998 *Appl. Phys. Lett.* **72** 2466
[7] Yang W, Vispute R D, Choopun S, *et al*. 2001 *Appl. Phys. Lett.* **78** 2787
[8] Li Z, Wang P, He J, *et al*. 2017 *Superlattices and Microstructures* **111** 852
[9] Makino T, Segawa Y, Kawasaki M, *et al*. 2001 *Appl. Phys. Lett.* **78** 1237
[10] Ohtani K, Belmoubarik M and Ohno H 2009 *J. Crystal Growth* **311** 2176
[11] Orphal L, Kalusniak S, Benson O, *et al*. 2017 *AIP Adv.* **7** 115309
[12] Xia C, Zhang H, An J, *et al*. 2014 *Phys. Lett. A* **378** 2251
[13] Allen M W, Miller P, Reeves R J, *et al*. 2007 *Appl. Phys. Lett.* **90** 062104
[14] Davis J A, Dao L V, Wen X, *et al*. 2008 *Nanotechnology* **19** 055205
[15] Belmoubarik M and El Moutaouakil A 2023 *J. Alloys Compd.* **941** 168960
[16] Thongnum A, Sa-Yakanit V and Pinsook U 2011 *J. Phys. D: Appl. Phys.* **44** 325109
[17] Yano M, Hashimoto K and Fujimoto K, *et al.* 2007 *J. Crystal Growth* **301–302** 353
[18] Bretagnon T, Lefebvre P, Guillet T, *et al*. 2007 *Appl. Phys. Lett.* **90** 201912
[19] Morhain C, Bretagnon T, Lefebvre P, *et al*. 2005 *Phys. Rev. B* **72** 241305
[20] Stölzel M, Kupper J, Brandt M, *et al.* 2012 *J. Appl. Phys.* **111** 063701
[21] Park S H and Ahn D 2005 *Appl. Phys. Lett.* **87** 253509
[22] Zhu L and Wang Z L 2019 *J. Phys. D: Appl. Phys.* **52** 343001
[23] Dai X, Hua Q, Sha W, *et al*. 2022 *J. Appl. Phys.* **131** 010903
[24] Dan M, Hu G, Nie J, *et al.* 2021 *Small* **17** e2008106
[25] Huang X, Du C, Zhou Y, *et al*. 2016 *ACS Nano* **10** 5145
[26] Funato M and Kawakami Y 2008 *J. Appl. Phys.* **103** 093501
[27] Belmoubarik M, Ohtani K and Ohno H 2008 *Appl. Phys. Lett.* **92** 191906
[28] Matsui H, Hasuike N, Harima H, *et al*. 2008 *J. Appl. Phys.* **104** 094309
[29] Cingolani R, Botchkarev A, Tang H, *et al*. 2000 *Phys. Rev. B* **61** 2711
[30] Wan S P, Xia J B and Chang K 2001 *J. Appl. Phys.* **90** 6210
[31] Kaminska A, Koronski K, Strak P, *et al*. 2020 *J. Appl. Phys.* **128** 050901
[32] Teisseyre H, Kaminska A, Birner S, *et al*. 2016 *J. Appl. Phys.* **119** 215702
[33] Grandjean N, Damilano B, Dalmasso S, *et al*. 1999 *J. Appl. Phys.* **86** 3714
[34] Chuang S 1996 *IEEE J. Quantum Electron.* **32** 1791
[35] Ridley B K, Schaff W J and Eastman L F 2003 *J. Appl. Phys.* **94** 3972
[36] Saha S and Kumar J 2016 *J. Comput. Electron.* **15** 1531
[37] Hedin L and Lundqvist B I 1971 *J. Phys. C: Solid State Phys.* **4** 2064
[38] Chuang S L and Chang C S 1996 *Phys. Rev. B* **54** 2491
[39] Fan W J, Abiyasa A P, Tan S T, *et al*. 2006 *J. Crystal Growth* **287** 28
[40] Winkelnkemper M, Schliwa A and Bimberg D 2006 *Phys. Rev. B* **74** 155322
[41] Sacconi F, Di Carlo A, Lugli P, *et al*. 2001 *IEEE Trans. Electron Dev.* **48** 450
[42] Chenini L, Aissat A and Vilcot J P 2019 *Superlattices and Microstructures* **129** 115
[43] Ashrafi A 2010 *J. Appl. Phys.* **107** 123527
[44] Kobiakov I B 1980 *Solid State Commun.* **35** 305
[45] Hu Y, Klein B D, Su Y, *et al*. 2013 *Nano Lett.* **13** 5026
[46] He J, Wang P, Chen H, *et al*. 2016 *Appl. Phys. Express* **10** 011101
[47] Moudou L H, Al-Hattab M, Rahmani K, *et al*. 2024 *J. Luminescence* **275** 120727
[48] Kuo Y H, Lee Y K, Ge Y, *et al*. 2005 *Nature* **437** 1334
[49] Robinson J W, Rice J H, Lee K H, *et al*. 2005 *Appl. Phys. Lett.* **86** 213103
[50] Gruber T, Kirchner C, Kling R, *et al*. 2004 *Appl. Phys. Lett.* **84** 5359
[51] Liu N, Hu G, Dan M, *et al*. 2019 *Nano Energy* **65** 104091
[52] Meng B, Tamayo-Arriola J, Le Biavan N, *et al*. 2019 *Phys. Rev. Appl.* **12** 054007
[53] Liu X Y, Holmström P, Jänes P, *et al*. 2007 *Phys. Status Solidi (b)* **244** 2892